Sequential Multimaterial Additive Manufacturing of Functionally Graded Biopolymer Composites

As Published: 10.1089/3DP.2020.0171

Publisher: Mary Ann Liebert Inc

Persistent URL: https://hdl.handle.net/1721.1/135200

Version: Final published version: final published article, as it appeared in a journal, conference proceedings, or other formally published context

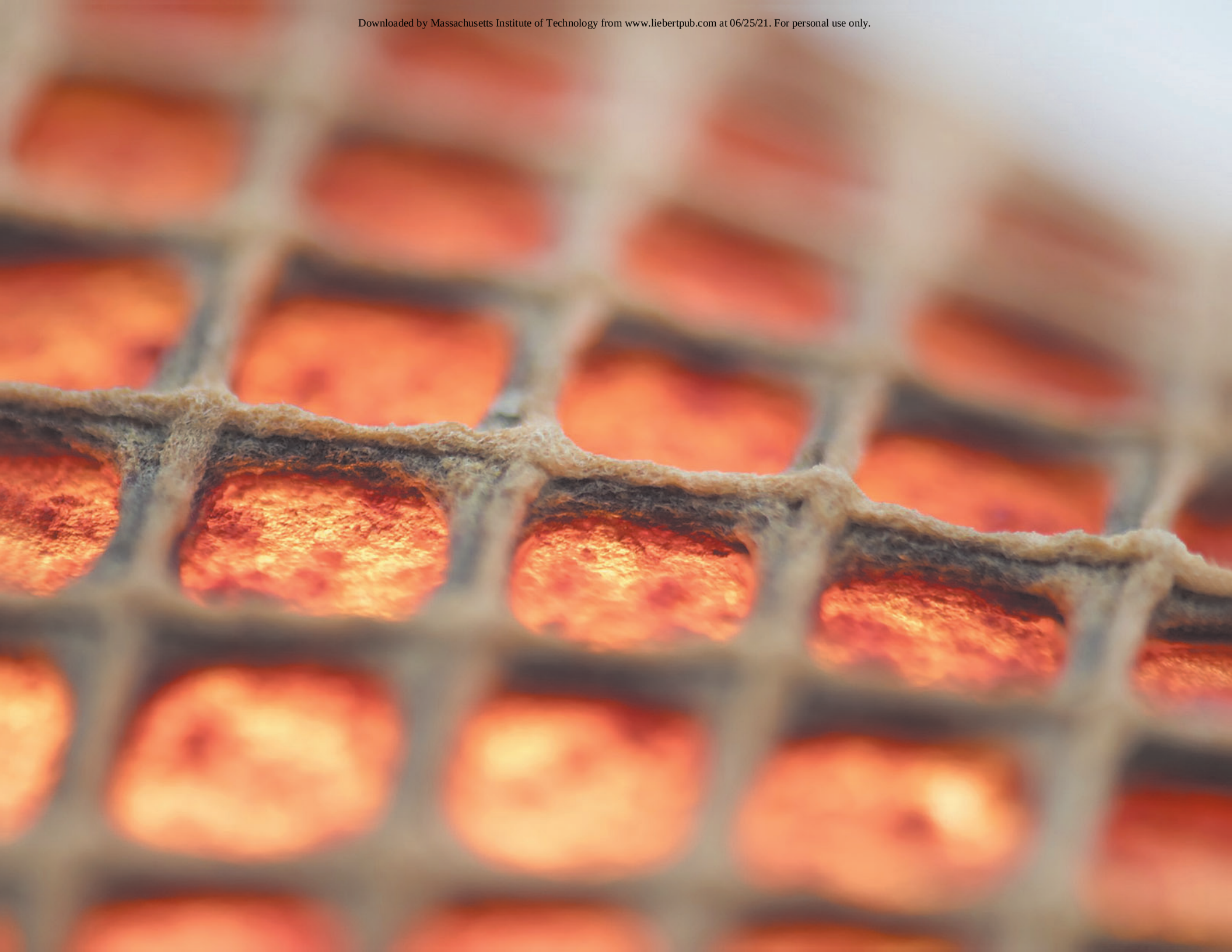

3D PRINTING AND ADDITIVE MANUFACTURING
Volume 7, Number 5, 2020

DOI: 10.1089/3dp.2020.0171

ORIGINAL ARTICLE

Sequential Multimaterial Additive Manufacturing of Functionally Graded Biopolymer Composites

Nic A. Lee, Ramon E. Weber,* Joseph H. Kennedy,* Josh J. Van Zak, Miana Smith, Jorge Duro-Royo, and Neri Oxman

Abstract

Cellulose, chitin, and pectin are three of the most abundant natural materials on Earth. Despite this, large-scale additive manufacturing with these biopolymers is used only in limited applications and frequently relies on extensive refinement processes or plastic additives. We present novel developments in a digital fabrication and design approach for multimaterial three-dimensional printing of biopolymers. Specifically, our computational and digital fabrication workflow—sequential multimaterial additive manufacturing—enables the construction of biopolymer composites with continuously graded transitional zones using only a single extruder. We apply this method to fabricate structures on length scales ranging from millimeters to meters. Transitional regions between materials created using these methods demonstrated comparable mechanical properties with homogenous mixtures of the same composition. We present a computational workflow and physical system support a novel and flexible form of multimaterial additive manufacturing with a diverse array of potential applications.

Keywords: biopolymers, additive manufacturing, functionally graded materials, chitosan, cellulose, pectin, hydrogels

Introduction and Background

Biopolymer additive manufacturing has gained traction as a sustainable alternative to conventional plastic production.[1] While recent advances have shown promise in creating structural composites from biopolymers, these methods are frequently limited in scale, require extensive refinement processes, or produce outputs with limited biodegradability.[2] In this research, we leverage the innate characteristics of water-soluble biopolymers to create functionally graded structures with continuous material property transitions, eliminating the need for synthetic binding agents and advanced equipment such as coaxial extrusion and multiple print chambers.

Smooth and continuous gradation of transitional zones has arisen as a common challenge in the manufacturing of functionally graded materials.[3] Multimaterial printing processes typically require each integrated material to be dithered, resulting in heterogeneous transitional zones with localized regions of each material.[4,5] In bioprinting and limited other applications, coaxial multichamber extruders are able to blend materials on the fly.[6] However, differences in factors such as extruded material viscosities and distance between material chambers and the extrusion nozzle[7] make it challenging to achieve precise material ratios. Our aim is to bypass these limitations by using a single extruder to create three-dimensional (3D)-printed biopolymer structures with the following characteristics: (1) tunable material property gradients with precise spatial control of specified material ratios, (2) efficacy across length scales ranging from millimeters to meters, and (3) composition of abundant biodegradable polymers.

While the additive manufacturing of hydrogel and biopolymer composites has been most broadly used in biomedical applications such as tissue engineering and cell scaffolding,[8] this article builds upon prior work in water-based digital fabrication. Specifically, the robotic 3D printing of large-scale, biopolymer composite (biocomposite) structures demonstrated additive manufacturing of hierarchical structures with discrete material transitions and blended

Media Lab, Massachusetts Institute of Technology, Cambridge, Massachusetts, USA.
*Indicates that these authors contributed equally.

Opposite page: A 3D printed biocomposite containing pectin, chitosan, and cellulose. *Photo credit:* The Mediated Matter Group.

multimaterial prints using coaxial extrusion and deacetylated chitin (chitosan) hydrogels.[9,10] In these examples, coaxial extrusion enabled the gradation of chitosan concentrations but was limited to small-scale artifacts and a set number of input materials. Conversely, hierarchically distributing chitosan concentrations allowed for the creation of large-scale, multimaterial composites, but material transitions were discrete. In addition, the relatively poor shape-retention properties of pure chitosan limited fabricated geometries to oriented line networks. Here, we expand this system to include cellulose and pectin hydrogel printing in multimaterial composites that are both large scale (1×2 m) and can contain continuous transitions between any number of materials.

Chitin and cellulose[11,12] comprise the most abundant biopolymers on earth. Their abundance is nature's evidence that these materials enhance biocompatibility and biodegradability, unlike many synthetic polymers. This abundance and biodegradability have served as primary drivers for the growing interest in chitosan-based composites as green materials for construction, but the relatively poor shape-retention and mechanical properties have necessitated the use of additives such as cellulose.[13] Hydrogels containing chitosan and cellulose have been used in a large-scale, additive manufacturing setting to great effect, enabling the creation of lightweight structures with impressive structural integrity.[14] However, multimaterial transitions are yet to be included in such systems.

Pectins are a common class of polysaccharides and are a secondary component of cell walls in terrestrial plants.[15] Many sources of pectin, such as from apples, are available in bulk and readily disperse into hydrogels when combined with water. Hydrogels containing pectin and chitosan have been applied for tissue-engineering applications,[16] while cellulose additives have enabled its use in small-scale additive manufacturing.[17] In addition, pectin's biocompatibility and abundance in foods such as fruits have led to its use in experimental food-printing processes.[18]

Chitosan is refined in bulk from waste generated by the shellfishing industry.[19] Shrimp shells are powdered and treated with acid and base solutions to dissolve calcium carbonate and isolate solubilized proteins. Apple pectin is extracted from pomace, a primary by-product of apple juice production, using high-temperature treatment and mineral acids.[20] Microcrystalline cellulose can be refined from agricultural waste through the spray-drying aqueous slurry that results from the hydrolysis of cellulose.[21] Each of the primary biopolymers used in the composites described here therefore shares the common characteristic of being refined in bulk from abundant waste streams.

Expanding the demonstrated ability of water-based digital fabrication to enable the creation of rigid, biodegradable composites, the work described here centers on the use of low-viscosity hydrogels to print flexible composites. Hydrogel mixtures are prepared from various ratios of these materials with each component influencing specific properties of the resulting composite, in proportion to its local presence. Chitosan enhances strength and stiffness, cellulose improves flexibility and strength, and pectin concentration directly relates to viscosity and ultimately, membrane thickness. We demonstrate that using geometric features at a 1 mm length scale, we are able to fabricate functionally graded composites with no visible transitional artifacts at $40\times$ magnification. In combination, these capabilities comprise a system that enables the high-resolution gradation of an unlimited number of water-soluble biopolymers using only a single extruder and abundant, biodegradable materials.

Materials and Methods

Hardware

A three-axis numerical control system was constructed for this study. It comprised two stepper motors devoted to Y-axis travel at a maximum resolution of 0.1 mm, one stepper motor devoted to X-axis travel at a maximum resolution of 0.1 mm, and one stepper motor devoted to Z-axis travel at a maximum resolution of 0.26 mm. The system's maximum travel range was set to $400 \times 300 \times 50$ cm in the X, Y, and Z dimensions, respectively.

An end effector, illustrated in Figure 1A, was designed with a single pneumatic extruder and interchangeable nozzles of varying diameter. The end effector housed a 300 mL cartridge that could be replaced independently of other system components. Nozzles of 1.024–1.628 mm diameter were affixed directly to cartridges. Wider nozzles were used for materials with greater viscosity. Pressure was varied with nozzle diameter to standardize material extrusion rates. This system could be affixed to an industrial robot as in Figure 1B for precision applications or to a computer numerical control (CNC) gantry as in Figure 1C for lower cost operations.

A compressed air source was regulated to an initial pressure of 345 kPa. Binary pressure regulation was provided by a solenoid valve to reduce lag times in the initiation and termination of extrusion. A secondary regulator was programmed to interpret fabrication information in the form of G-code spindle-speed commands and regulate pressure at 0–340 kPa. To reduce lag time in pressure changes, pressure data for a portion of upcoming points in a toolpath were preloaded from streamed data. The system retained the ability to provide real-time overrides to pressure and feed rate for these preloaded data.

Material composition

Aqueous biopolymers were prepared as hydrogel solutions primary composed of three base components: 85% deacetylated chitosan (VWR©, Radnor PA), microcrystalline cellulose (VWR), and apple pectin (VWR). Chitosan-based solutions were prepared by dissolving chitosan powder in 1% (v/v) glacial acetic acid (VWR). Relative amounts of chitosan, cellulose, and pectin were varied according to the desired properties of the dried composite material.

Pectin was used to form hydrogel bases with concentrations ranging from 18% to 40% (w/v). Concentrations above 40% yielded hydrogels that did not homogenize. At midrange concentrations (28–32%), pectin provided a convenient base for the incorporation of both chitosan and cellulose. Without these additions, pectin hydrogels dried into flexible membranes.

Chitosan concentrations ranged from 3% to 8% (w/v). Enough protonatable groups are present in 85% deacetylated chitosan to allow for its dispersion in low-concentration acetic acid solutions, forming a gel. At concentrations above 8%, chitosan additions led to significant deformation in dried composites and were therefore not suitable for fabrication.

Microcrystalline cellulose was incorporated in concentrations ranging from 5% to 20% (w/v). This additive was not used independently to form hydrogels, but rather was

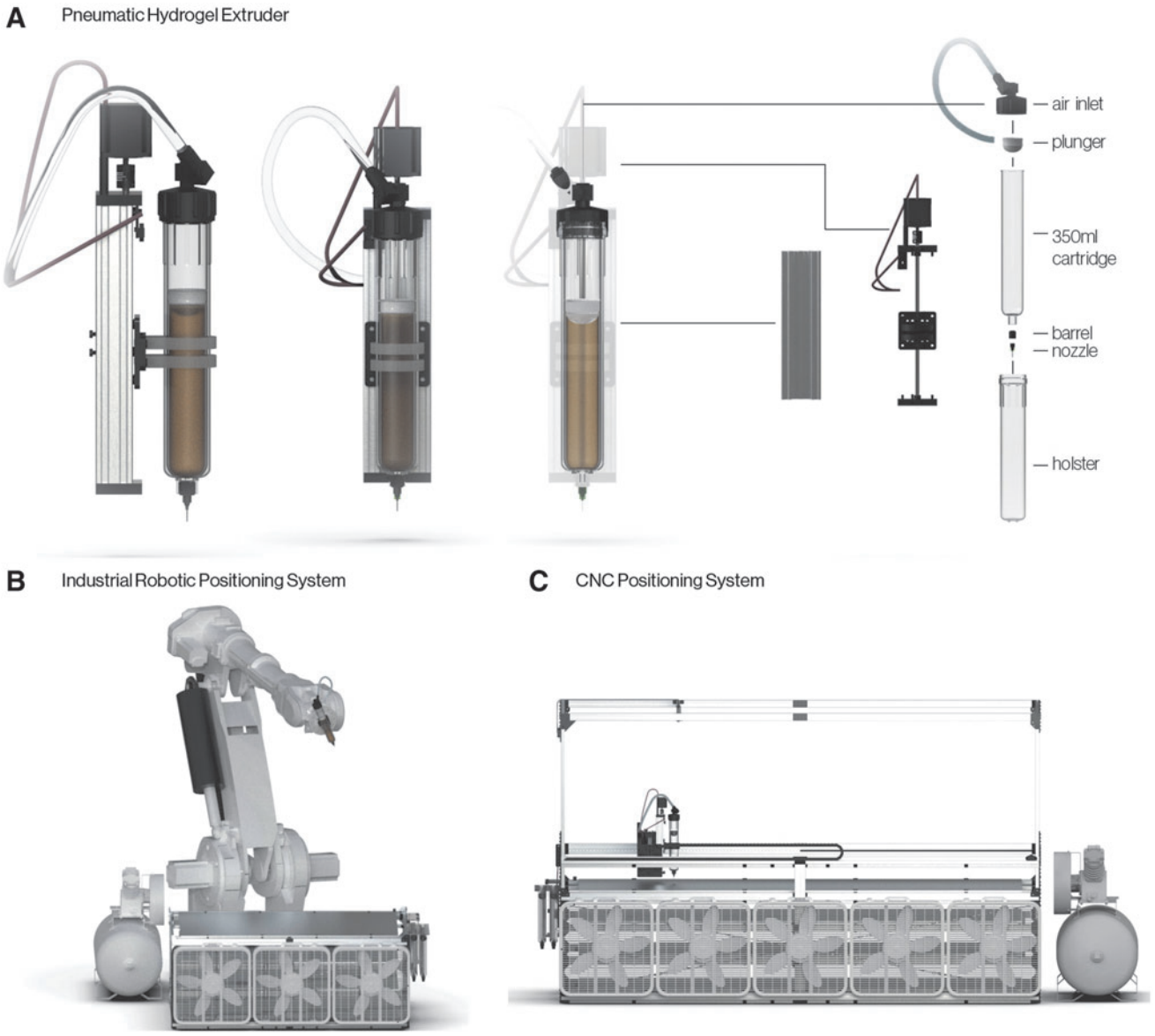

FIG. 1. Hardware specifications for a numerically controlled system for sequential multimaterial additive manufacturing. The extruder consists of a removable cartridge with interchangeable nozzles inserted into a holster. Z-axis movement is controlled via a linear actuator, while pneumatic extrusion is driven by compressed air with pressure regulated by a digital controller **(A)**. The system can be affixed to a 6-axis industrial robot for high-precision applications **(B)** or to a CNC gantry with 3-axes of travel **(C)**. In both systems, extrusion-nozzle diameter and pneumatic pressure can be adapted according to the viscosity of extruded hydrogels. A fan array can be used to accelerate hydrogel drying.

incorporated as an additive to pectin and chitosan solutions. Concentrations above 20% did not incorporate into hydrogels, resulting in dried composites that tore or had impaired structural integrity.

Dynamic viscosity was measured for each hydrogel immediately after homogenization using an AR-G2 rotational viscometer (TA Instruments, Newcastle DE) with a 60 mm 2° cone-and-plate geometry at 25°C. Shear rates were swept from 6 rpm to 60 rpm. Tensile testing was conducted using an Instron 5984 (Instron, Norwood, MA) with a 20,000 kg maximum load and a trigger load of 2N. All composites were tested to failure under tension at a test speed of 0.2 mm/min.

Six hundred milliliters of hydrogel solutions were homogenized using an industrial blender (Blendtec©, Orem UT). Biopolymers were incorporated into water at 25°C in the following order: pectin, chitosan, cellulose, acetic acid. Solutions were blended until homogeneous and immediately transferred to 300 mL cartridges for extrusion.

These biopolymers were mixed to create colloid gels that were then printed at 25°C and 30% humidity. By spatially templating extrusion pressure, the amount of material deposited at each location was precisely specified. Subsequent layers of printed material were similarly graded according to the desired material properties at each point. In this way, multiple materials were extruded atop one another in sequence. Figure 2A displays the resultant printed biocomposite with linearly graded proportions of chitosan created by printing the toolpaths shown in Figure 2B. Extruded

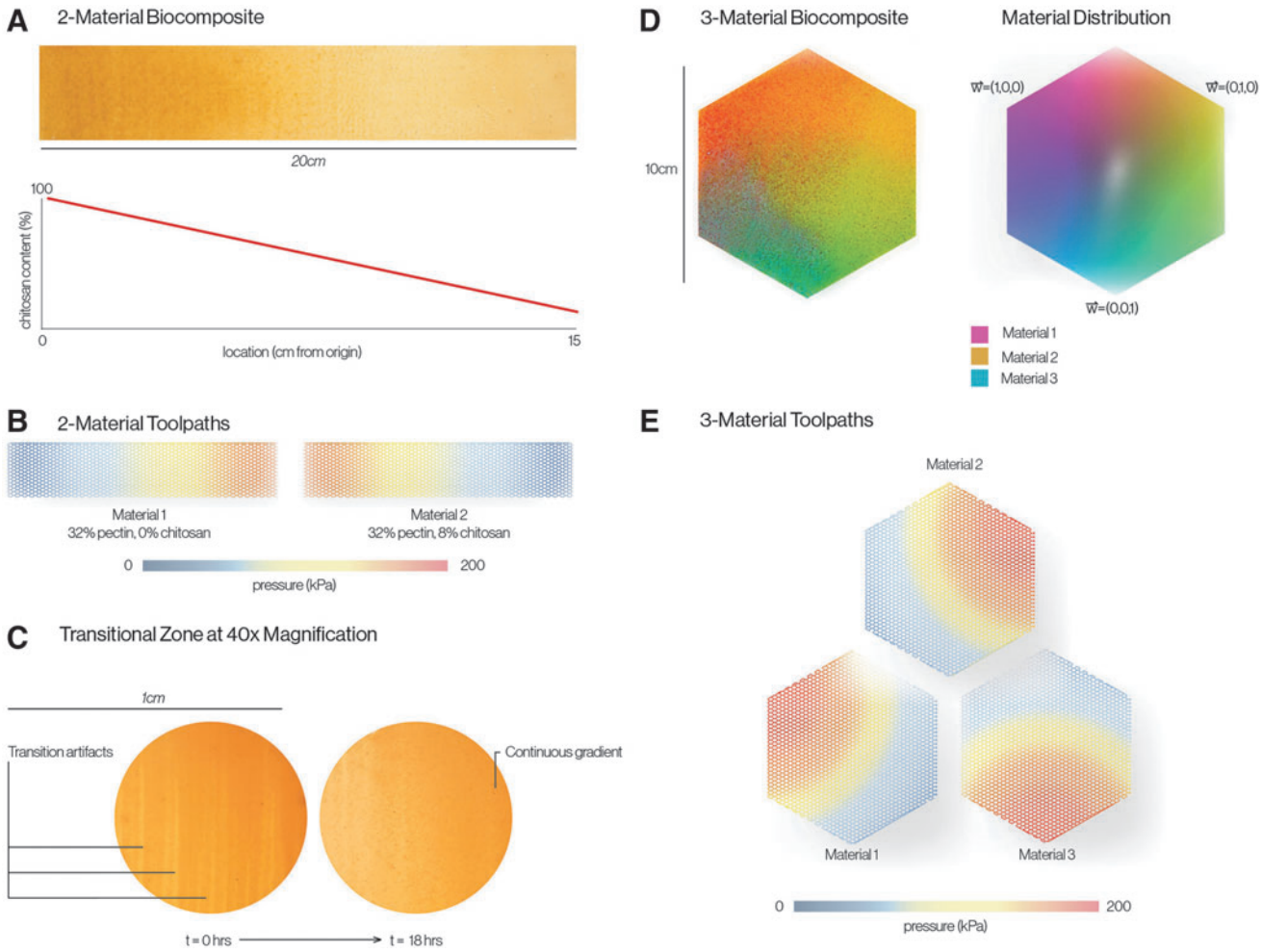

FIG. 2. Linear gradation of two and three dissimilar hydrogel solutions within individual composites. Mechanical properties are graded according to the linear gradation of chitosan concentration across a printed composite **(A)**. The composite is fabricated through the sequential extrusion of pectin hydrogels containing 0% and 8% chitosan by varying the extrusion pressure of two toolpaths printed sequentially **(B)**. Transitional regions at 40× magnification do not maintain their originally printed transitional artifacts, but diffuse into continuous gradients **(C)**. A printed composite containing dyed hydrogels demonstrates gradation with more than two materials where a weight vector w specifies the amount of each material at each location **(D)**. Sequential multimaterial additive manufacturing flexibly accommodates any number of materials as material distributions are normalized and assigned pressure values across toolpaths to ensure an equal total material presence at each location **(E)**.

hydrogels dried via evaporation, providing a period of time in which the solute was able to locally diffuse and create continuous gradients, shown in Figure 2C, due to the innate properties of water-soluble biopolymer hydrogels.[22] The extent of diffusion varied as a function of ambient temperature and humidity or by duration between material additions.

Computational workflow

The computational system was designed to translate mesh representations of geometry, with embedded metadata corresponding to material proportions, into machine parameters for extrusion toolpaths. Meshes were designed in a computer-aided design (CAD) environment as either two-dimensional (2D) or 3D geometric representations of the desired object. Three-dimensional mesh objects were sliced into layers for additive manufacturing. Each point of the mesh objects contained XYZ spatial data as well as a user-defined 1 by n vector $w(n)$ in which the relative weight, or proportion of each print material, was encoded, where n is equal to the total number of distinct materials created for extrusion in a single print. Figure 2D illustrates the resulting multimaterial print (right) from a user-defined mesh (left) where weight values are mapped to colors.

Two-dimensional slices of mesh objects were infilled using a hexagonal toolpath with an edge length of 0.5 mm. Weight vectors were assigned to each point in the toolpath from metadata representing the desired distribution of each material, with 1 representing maximum presence of the material and 0 representing its absence. Once weights had been assigned to each component of the weight vector, the vector was normalized to ensure the extrusion of an equal total amount of material at each point. Therefore, each component of $w(n)$ contained a scalar value from 0 to 1 that represented the relative proportion of the material to be extruded at that location.

A unique toolpath was generated for each material, excluding points where $w(n)=0$ to reduce fabrication time. Infills were generated by taking the concave hull of the set of mesh points to be printed and infilling the 2D boundary with portions of the pre-established hexagonal toolpath. Toolpaths were iteratively linked and connected through their shared boundaries. Discrete infilled sections were joined by linear paths with weight values of zero. As illustrated in Figure 2E, a single execution of the system then outputs a sequence of n toolpaths that infilled the designed mesh object and contained spatial data, feed rates, and relative weight values for each material.

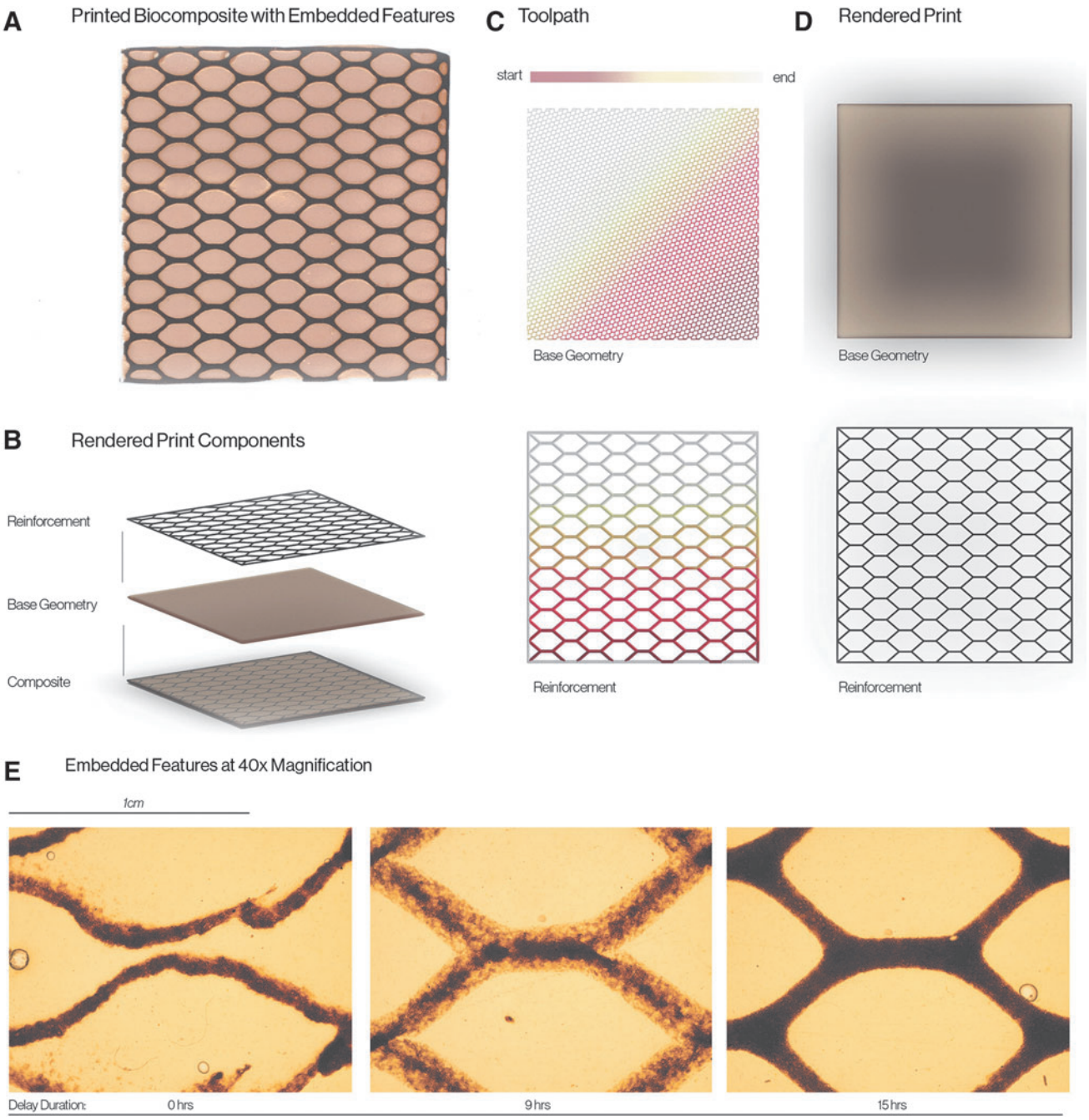

FIG. 3. Sequential additive manufacturing can be used to create composites with embedded secondary geometries at the resolution of 1mm such as the pictured biocomposite **(A)**. Base and embedded geometries are defined as discrete objects composed of different materials **(B)**. Fabrication information consisting of the toolpath, feed rate, and extrusion pressure is generated as they are for prints with graded transitions **(C)** and anticipated outputs can be rendered from this information **(D)**. Relatively low viscosity in the base layer leads to the formation of a continuous membrane, while high-viscosity reinforcement materials retain their printed geometry. **(E)** The amount of diffusion experienced by the reinforcement geometry is dependent on the duration that the base layer has been allowed to dry before printing the next layer. Providing adequate time for the base layer to partially dry enables the preservation of high-resolution features in the reinforcement pattern.

Relative weight values were then remapped to preestablished experimentally derived minimum and maximum extrusion pressures. Minimum values represented the highest pressure at which no material was extruded, while maximum pressures represented the lowest pressure at which a line of 1 mm diameter could be continuously extruded. The proportion of extruded material was estimated to scale linearly, with a scalar weight value of 0.5 resulting in an approximate extrusion diameter of 0.5 mm, and therefore, intermediate pressures were assigned via linear interpolation. The rate of this extrusion was manually varied with material viscosity, feed rate, and nozzle diameter.

Transitional zones were monitored by printing 20 cm by 4 cm samples with linear transitions between two materials. Immediately after printing, samples were placed under a Wild M420 photomacroscope (Wild, Heerbrugg, Switzerland) and photographed every 5 min for 24 h at 40× magnification. Images were centered on regions with clear transitional artifacts, recognizable as discrete streaks of input materials. Ambient conditions were maintained at 25°C and 40% humidity during the monitoring period. Images were then reviewed to select the first time stamp at which transitional artifacts had diffused into continuous gradients.

Environmental control and postfabrication

Extruded hydrogels were allowed to dry at temperatures of 20–26°C and 10–70% humidity to form composites. The drying time allowed solute to locally diffuse, creating distributions of material at a finer resolution than was printed. Lower temperature or higher humidity corresponded to increased drying time, which allowed for a greater degree of diffusion, resulting in finer material gradients.

Increasing the period of time between subsequent material layers, or delay duration, reduced the level of interlayer diffusion, and therefore, the presence of material gradients in the dried composite. This capability was leveraged to create discrete transitions between materials of different properties, such as the printed composite in Figure 3A. Such prints require the user to separately design a ''base'' geometry and an ''embedded'' pattern as in Figure 3B. Figure 3C illustrates the translation of these designs and their rendered outputs (Fig. 3D) into fabrication data, which follows the same computational pipeline as designs with graded transitions. With precise timing, secondary materials can be embedded into a composite without dispersion or causing macroscale changes to the surface characteristics of the composite. In Figure 3E, photomacroscope analysis of prints with features embedded within a low-viscosity base illustrates the impact of different drying periods on the integrity of the embedded features. For a 32% (w/v) pectin base, 15 h of drying at 25°C and 40% humidity enabled feature preservation of an embedded hydrogel containing 32% (w/v) pectin, 8% (w/v) chitosan, 10% (w/v) microcrystalline cellulose, and 1% (v/v) acetic acid.

Results

Table 1 illustrates the relationships between each hydrogel component and the resultant mechanical properties of printed composites under tension. Higher concentrations of chitosan led to corresponding increases in ultimate tensile strength and stiffness. Increased cellulose concentrations in composites containing chitosan demonstrated markedly increased stiffness, but had a minimal impact on ultimate tensile strength. A less dramatic increase in stiffness resulted from the addition of 10% (w/v) microcrystalline cellulose to composites not containing chitosan. These results suggest a potential interaction between microcrystalline cellulose and chitosan that leads to significant increases in composite stiffness.

Table 1. Mechanical Properties of Biopolymer Composites Vary According to Composition

Composition	*E* (N/m^2)	*Ultimate tensile stress* (N/mm^2)	*Elongation at break* (%)
32% pectin 0% chitosan 0% cellulose 1% acetic acid	23.70 (10^6)	7.03 (10^6)	27.33
32% pectin 4% chitosan 0% cellulose 1% acetic acid	129.72 (10^6)	9.86 (10^6)	10.50
32% pectin 8% chitosan 0% cellulose 1% acetic acid	442.10 (10^6)	11.67 (10^6)	4.36
32% pectin 8% chitosan 10% cellulose 1% acetic acid	894.65 (10^6)	10.83 (10^6)	1.72
32% pectin 0% chitosan 10% cellulose 1% acetic acid	40.79 (10^6)	5.01 (10^6)	16.00

All hydrogels demonstrated shear-thinning behavior, crucially enabling their pneumatic extrusion and subsequent shape retention. Each material's viscosity at low rotational velocities (6 rpm) provides an estimation of its behavior at low or zero extrusion pressure, while its viscosity at high rotational velocities (60 rpm) illustrates its behavior at higher extrusion pressures. This behavior is described in Table 2. Chitosan concentration correlated to hydrogel viscosity in pectin-based hydrogels containing acetic acid. An addition of 4% (w/v) chitosan notably increased hydrogel viscosity. Subsequently increasing this concentration to 8% (w/v) did not significantly increase hydrogel viscosity. Incorporating 5% (w/v) microcrystalline cellulose into composites containing chitosan led to a proportional increase in hydrogel viscosity and increased shear-thinning behavior. Further increases in viscosity were not observed when the microcrystalline cellulose concentration was increased to 10% (w/v).

Hydrogel mixtures containing 32% (w/v) pectin, 8% (w/v) chitosan, 10% (w/v) microcrystalline cellulose, and 1% (v/v) acetic acid exhibited a viscosity of 11.7 (10^{-2}) Pa.s at 60 rpm and required 340 kPa to be extruded through a 1.628-mm-diameter nozzle, resulting in an extrusion width of 1 mm. This pressure bordered the upper limits of the system's capacity. Extruding more viscous hydrogels would require either a higher maximum pressure or a wider nozzle diameter,

Table 2. Extrusion Pressure and Nozzle Diameter Are Determined by Hydrogel Viscosity at 25°C

Composition	*Hydrogel viscosity at 6 rpm (Pa.s)*	*Hydrogel viscosity at 60 rpm (Pa.s)*	*Shear-thinning ratio*	*Minimum extrusion pressure (kPa)*	*Maximum extrusion pressure (kPa)*	*Nozzle diameter (mm)*
32% pectin 0% chitosan 0% cellulose 0% acetic acid	7.27 (10^{-2})	1.18 (10^{-2})	6.16	0	68.0	1.024
32% pectin 4% chitosan 0% cellulose 1% acetic acid	54.9 (10^{-2})	16.9 (10^{-2})	3.25	34.5	138	1.290
32% pectin 8% chitosan 0% cellulose 1% acetic acid	56.3 (10^{-2})	18.7 (10^{-2})	3.01	68.0	207	1.290
32% pectin 8% chitosan 5% cellulose 1% acetic acid	134 (10^{-2})	8.64 (10^{-2})	15.5	103	241	1.628
32% pectin 8% chitosan 10% cellulose 1% acetic acid	123 (10^{-2})	11.7 (10^{-2})	10.4	207	340	1.628

the latter of which would result in lower resolution prints. Similarly, a lower limit was present in the extrusion of 32% (w/v) pectin solutions, which exhibited a viscosity of 7.72 (10^{-2}) Pa.s at 6 rpm and would begin extruding from a 1.024-mm-diameter nozzle at any nonzero pressure.

Photomacroscope observation of two-material-printed hydrogels at 40× magnification indicated that diffusion-based blending would blend discrete regions of up to 1 mm in length. In Figure 2D, transitional artifacts with a width of below 1 mm effectively form a gradient after 18 h at 25°C and 40% humidity, while artifacts greater than 1 mm in width remain visible in the dried composite. Diffusion-based hydrogel blending was found to occur most effectively when infill toolpaths were spaced at half of the extrusion width. In addition, transitional artifacts were observed to be less prevalent with a hexagonal infill as the one in Figure 2B and E was used rather than simple linear paths. This is likely due to the mechanical action of the extrusion nozzle assisting in blending adjacent paths.

Sequential multimaterial additive manufacturing allows for a level of material blending not found in conventional multimaterial printing methods.[23] The hydrogel nature of the extruded materials provides a matrix in which the solute can locally diffuse and blend. Beyond gradation, the system can be used to interpolate between the properties of blended materials. For example, a hydrogel containing no chitosan can be layered with a hydrogel containing 8% chitosan at a 3:1 ratio to obtain the properties of a hydrogel with 2% chitosan. In Table 3, the interpolated composite demonstrates equivalent mechanical and optical properties to homogenized hydrogels of the same concentrations. This capability unlocks access to a diverse array of material properties from a limited selection of mixtures.

The described methods encompass a comprehensive workflow from object definition to fabrication. Figure 4illustrates the full computational pipeline for this method, beginning with the user's definition of a multimaterial print in Figure 4A. This user-defined information is then used to generate normalized weight values in Figure 4B, which are remapped to experimentally derived minimum and maximum pressure values in Figure 4C. Figure 4D shows the sequential process of layering hydrogels to create a multimaterial composite.

Table 3. Comparison of Prehomogenized and Sequentially Blended Hydrogels

Composition	*E (N/m²)*	*Ultimate tensile stress (N/mm²)*	*Elongation at break (%)*
Material 1 32% pectin 0% chitosan 0% cellulose 1% acetic acid	23.70 (10^6)	7.03 (10^6)	27.33
Material 2 32% pectin 8% chitosan 0% cellulose 1% acetic acid	442.10 (10^6)	11.67 (10^6)	4.36
Transitional blend Material 1 (50%) Material 2 (50%)	137.28 (10^6)	9.82 (10^6)	8.21
Prehomogenized control 32% pectin 4% chitosan 0% cellulose 1% acetic acid	129.72 (10^6)	9.86 (10^6)	10.50

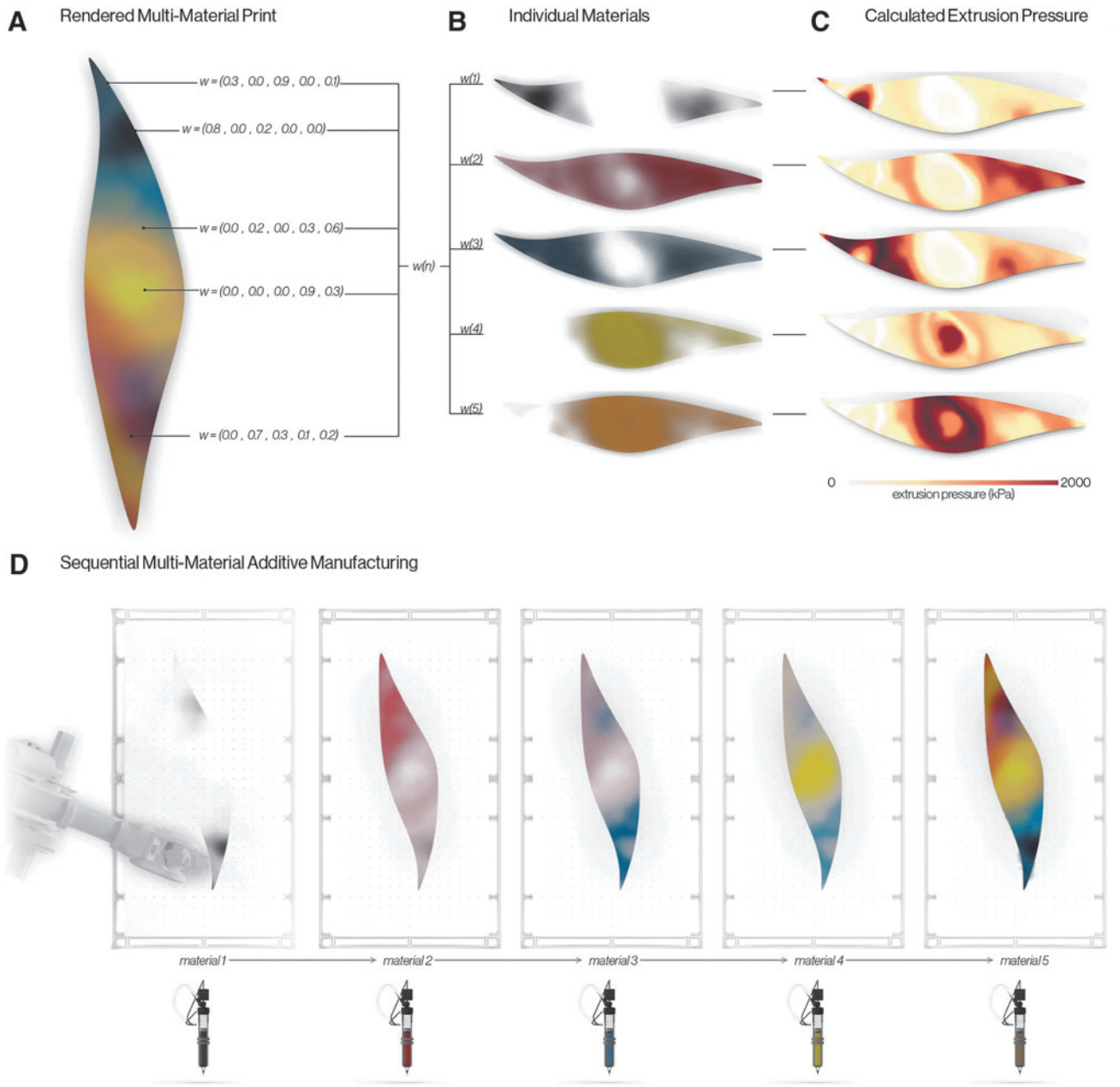

FIG. 4. Translation of a digital mesh object into machine parameters for sequential additive manufacturing. **(A)** The digital representation is encoded with metadata specifying the amount of material, designated by the weight value w at each point in a toolpath. Each weight value is stored in a vector and normalized to ensure an equal distribution of material at all points for each material **(B)**. Weight components are remapped to **(C)** machine data specifying extrusion pressure within a minimum and maximum range according to experimental data on the resulting extrusion width. Material-specific pressure values in the form of G-code commands are sent to a numerically controlled extrusion system **(D)**. The streamed data for pressure and feed rate can be manually overridden by the user during fabrication. Extruded hydrogel layers blend during evaporative drying to form graded composites.

Importantly, this workflow is agnostic to the scale of fabrication. To demonstrate the applications of this method at a large scale, the described computational pipeline was applied to a 5-m-tall structure clad with pectin-based biopolymer panels. The use of the computational pipeline to assign material values and generate digital assets is shown in Figure 5A. Figure 5B shows the CNC gantry used to fabricate the final product displayed in Figure 5C, which houses printed panels reaching up to 2 m in length with continuously graded and discrete transitions between materials.

Sequential multimaterial additive manufacturing enables the creation of continuously graded hydrogel scaffolds using a single extruder for the first time. The accessible nature of the implemented biopolymers coupled with the scalable functionality of the fabrication system enables high-precision small-scale and large-scale applications such as the creation of biodegradable cell-scaffolds or architectural elements.

FIG. 5. Fabrication of a large-scale prototypical membrane structure with both continuously graded and discrete embedded material transitions demonstrates efficacy of the described methods across scales of fabrication. A 5-m-tall base-geometry was processed into developable panels and assigned colored gradients of materials, as well as embedded reinforcement patterns, with the largest panel spanning 2 m **(A)**. The panelized structure was fabricated by affixing the described extrusion system to a 2 m by 4 m CNC gantry **(B)** and supported by a rigid acrylonitrile butadiene styrene (ABS) scaffold **(C)**. Base layers containing 32% pectin, 0% to 6% chitosan, and 1% acetic form a flexible skin with gradients of color and strength. A secondary network, embedded as a reinforcement pattern within the base layer, consists of 32% pectin, 8% chitosan, 15% cellulose, and 1% acetic acid and provides additional reinforcement to the structure. CNC, computer numerical control.

These advances demonstrate the potential for biopolymer printing to provide advanced functionality using relatively simple technology.

Discussion

The focus of the present work was to enable precise spatial control and material ratios in a simple scalable system for the fabrication of functionally graded biocomposite structures. A primary limitation of the described system is the challenge associated with vertical layering. The relatively low viscosity of the extruded hydrogels means that subsequent layering with the intention of increasing height often leads to the collapsing of base layers and loss of structural integrity. Adding fillers or crosslinking hydrogels to enable this function by necessity diminishes the capability for local diffusion to occur.

One possible solution to this limitation would be to increase the maximum pressure allowed by the system to enable the use of very high-viscosity hydrogel such as those used for 3D tissue scaffolds. This would enable further examination of the effectiveness of diffusion-based hydrogel blending between vertical layers. However, in a 3D setting, it is possible that gravity would play a more important role in the diffusion of solutes and that extended drying times may cause certain solutes to settle to lower layers.

While chitosan, cellulose, and pectin enable a wide range of material properties, a number of other biopolymers, including silk fibroin[24] and lignin,[25] could allow for stronger or more elastic regions in composites, and should be investigated. Gradation with these biopolymers could furthermore enable fine regional control of biocompatibility, dissociation rate, or fiber alignment. The integration of these biopolymers could therefore extend the utility of the described platform to additional disciplines and applications by providing biopolymers with analogous mechanical properties to rigid plastics or textiles.

Conclusions

Our results indicate that continuously graded hydrogel composites can be created using a single extruder and sequential multimaterial additive manufacturing. Hydrogels printed in this manner locally blend to form transitional regions with mechanical properties comparable with homogeneous mixtures of the materials in the transition. The presented workflow provides a mechanically simple means to achieve results that typically require multichamber coaxial extrusion.

Sequential multimaterial additive manufacturing enables a spectrum of functionally graded biopolymer composite designs based on the level of localized solute diffusion, as controlled by fabrication parameters. On one end of this spectrum, when diffusion is maximized, the system allows for the creation of continuous material gradients where the resolution of transitional features is limited by chemical, rather than mechanical, properties. On the other end, when diffusion is minimized, composites can be made to contain discrete material transitions and embedded high-resolution patterns. These capabilities are unique to additive manufacturing with water-soluble biopolymers and are conserved across scales of fabrication ranging from millimeters to meters. Furthermore, they can be used to integrate any number of materials with vastly different properties.

The presented methods encompass a remarkably simple and flexible platform for multimaterial additive manufacturing with the most common organic materials on Earth. This system augments biocomposites with capabilities not yet found in conventional plastics and demonstrates a simple means through which high-resolution multimaterial additive manufacturing can be achieved. With these capabilities, sequential multimaterial additive manufacturing sets a precedent for accessible, advanced digital fabrication.

Author Disclosure Statement

No competing financial interests exist.

Funding Information

This research was primarily sponsored by The Mediated Matter research group at the MIT Media Lab. Additional funding was provided by NOE. LLC, Stratasys Ltd., MIT Research Laboratory of Electronics, Wyss Institute at Harvard, Department of Systems Biology at Harvard, GETTY-LAB, Robert Wood Johnson Foundation, TBA-21 Academy, Thyssen-Bornemisza Art Contemporary, Stratasys Direct Manufacturing, National Academy of Sciences, San Francisco Museum of Modern Art, and the Esquel Group.

References

1. Liu J, Sun L, Xu W, *et al*. Current advances and future perspectives of 3D printing natural-derived biopolymers. Carbohydrate Polymers 2019;207:297–316.
2. Dai L, Cheng T, Duan C, *et al*. 3D printing using plant-derived cellulose and its derivatives: A review. Carbohydrate Polymers 2019;203:71–86.
3. Naebe M, Shirvanimoghaddam K. Functionally graded materials: A review of fabrication and properties. Appl Mater Today 2016;5:223–245.
4. Bandyopadhyay A, Heer B. Additive manufacturing of multi-material structures. Materials science and engineering R: Reports 2018;129:1–16.
5. Chmielewski M, Pietrzak K. Metal-ceramic functionally graded materials—Manufacturing, characterization, application. Bull Polish Acad Sci Tech Sci 2016;64:151–160.
6. Ozbolat IT, Chen H, Yu Y. Development of ''Multi-arm Bioprinter'' for hybrid biofabrication of tissue engineering constructs. Robot Comput Integrat Manufact 2014;30:295–304.
7. Liu W, Zhang YS, Heinrich MA, *et al*. Rapid continuous multimaterial extrusion bioprinting. Adv Mater 2017;29.
8. Billiet T, Vandenhaute M, Schelfhout J, *et al*. A review of trends and limitations in hydrogel-rapid prototyping for tissue engineering. Biomaterials 2012;33:6020–6041.
9. Mogas-Soldevila L, Duro-Royo J, Oxman N. Water-based robotic fabrication: Large-scale additive manufacturing of functionally graded hydrogel composites via multi-chamber extrusion. 3D Print Addit Manufact 2016;1:141–151.
10. Duro-Royo J, Mogas-Soldevila L, Oxman N. Flow-based fabrication: An integrated computational workflow for design and digital additive manufacturing of multifunctional heterogeneously structured objects. Computer Aided Design 2015;69:143–154.
11. Klemm D, Heublein B, Fink HP, *et al*. Cellulose: Fascinating biopolymer and sustainable raw material. Angewandte Chem 2005;44:3358–3393.
12. Roberts GAF, Roberts GAF. Preparation of Chitin and Chitosan. In: Chitin Chemistry, Springer, 1992; (pp. 54–84). https://doi.org/10.1007/978-1-349-11545-7_2
13. HPS, A. K., Saurabh CK, Adnan AS, *et al*. A review on chitosan-cellulose blends and nanocellulose reinforced chitosan biocomposites: Properties and their applications. Carbohydrate Polymers. 2016;150:216–226.
14. Sanandiya ND, Vijay Y, Dimopoulou M, *et al*. Large-scale additive manufacturing with bioinspired cellulosic materials. Sci Rep 2018;8:1–8.
15. Rinaudo M. Chitin and chitosan: Properties and applications. Prog Polymer Sci 2006;31:603–632.
16. Noreen A, Akram J, Rasul I, *et al*. Pectins functionalized biomaterials; a new viable approach for biomedical applications: A review. Int J Biol Macromol 2017;101:254–272.

17. Sundarraj AA, Ranganathan TV. Comprehensive review on cellulose and microcrystalline cellulose from agro-industrial wastes. Drug Invention Today 2018;10:2783–2788.
18. Wikiera A, Mika M, Starzyńska-Janiszewska A, *et al*. Endo-xylanase and endo-cellulase-assisted extraction of pectin from apple pomace. Carbohydrate Polymers 2016;142:199–205.
19. Martins JG, Camargo SE, Bishop TT, *et al*. Pectin-chitosan membrane scaffold imparts controlled stem cell adhesion and proliferation. Carbohydrate Polymers 2018;197:47–56.
20. Cernencu AI, Lungu A, Stancu IC, *et al*. Bioinspired 3D printable pectin-nanocellulose ink formulations. Carbohydrate Polymers 2019;220:12–21.
21. Feng C, Zhang M, Bhandari B. Materials properties of printable edible inks and printing parameters optimization during 3D printing: A review. Crit Rev Food Sci Nutr 2019;59:3074–3081.
22. Amsden B. Solute diffusion within hydrogels. Mechanisms and models. Macromolecules 1998;31:8382–8395.
23. Loh GH, Pei E, Harrison D, *et al*. An overview of functionally graded additive manufacturing. Addit Manufact 2018;23:34–44.
24. Numata K, Yamazaki S, Katashima T, *et al*. Silk-pectin hydrogel with superior mechanical properties, biodegradability, and biocompatibility. Macromol Biosci 2014;14:799–806.
25. Thakur VK, Thakur MK. Recent advances in green hydrogels from lignin: A review. Int J Biol Macromol 2015;72:834–847.

Address correspondence to:
Neri Oxman
Media Lab
Massachusetts Institute of Technology
Cambridge, MA 02139-4307
USA

E-mail: neri@mit.edu